[Supplementary Material]

Chariots in the Eurasian Steppe: a Bayesian approach to the emergence of horse-drawn transport in the early second millennium BC

Stephan Lindner*

* *Institut für Prähistorische Archäologie, Freie Universität Berlin, Germany (✉ stephan.lindner@slovoscript.de)*

Table S1. The model in OxCal v4.3 with two phases for the radiocarbon determinations from KA-5. Here, a direct chronological relationship between the phases is assumed, based on typological arguments between the earlier graves in kurgan 2 and the later graves in kurgan 4 (Hanks *et al.* 2007;Bronk Ramsey 2009). The calibration curve of Reimer *et al*. (2013) was used to calibrate the results. All dates have been rounded to the closest ten.

	Unmodeled (BC)				Modelled (BC)			
	68.2%		95.4%		68.2%		95.4%	
	From	To	From	To	From	To	From	To
Start Phase 1					1960	1900	2020	1890
OxA-12530	1960	1890	2020	1780	1930	1890	1960	1880
OxA-12533	1950	1790	2010	1770	1930	1890	1950	1880
OxA-12532	2020	1920	2040	1890	1940	1890	1970	1880
OxA-12531	1940	1780	1970	1770	**1930**	**1890**	**1950**	**1880**
Transition Phase 1 / 2					1920	1880	1940	1840
OxA-12534	1920	1780	1940	1760	1900	1820	1910	1780
OxA-12650	1900	1770	1930	1760	1900	1820	1910	1780
OxA-12535	1880	1770	1920	1700	1900	1830	1910	1780
End Phase 2					1890	1800	1910	1700

Table S2. The radiocarbon dates from KA-5 within one phase in OxCal v4.3 (Hanks *et al.* 2007; Bronk Ramsey 2009). The calibration curve of Reimer *et al*. (2013) was used to calibrate the results. All dates have been rounded to the closest ten.

	Unmodeled (BC)				Modelled (BC)			
	68.2%		95.4%		68.2%		95.4%	
	From	To	From	To	From	To	From	To
Start of radiocarbon series					1950	1890	2010	1880
OxA-12530	1960	1890	2020	1780	1920	1890	1960	1880
OxA-12533	1950	1790	2010	1770	1920	1880	1950	1830
OxA-12532	2020	1920	2040	1890	1930	1890	1970	1880
OxA-12531	1940	1780	1970	1770	**1920**	**1880**	**1950**	**1820**
OxA-12534	1920	1780	1940	1760	1920	1880	1940	1820
OxA-12650	1900	1770	1930	1760	1920	1880	1940	1820
OxA-12535	1880	1770	1920	1700	1920	1870	1940	1810
End of radiocarbon series					1910	1850	1920	1750

Sensitivity analysis for the modelled date probabilities of burial 8 with an early chariot at KA-5.

A) Model with two phases

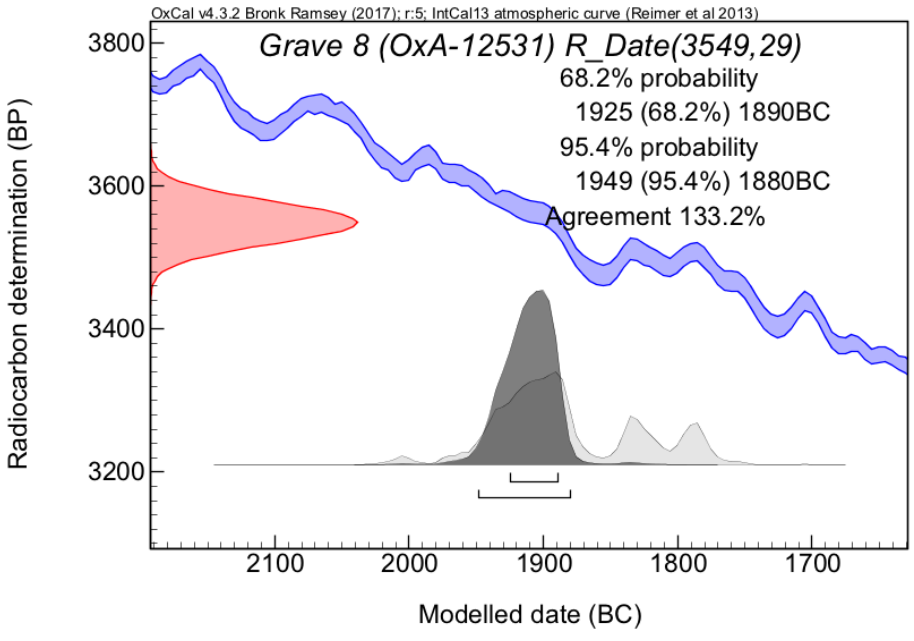

Figure S1. Model with two phases. The modelled probable age range based on the separation of the radiocarbon dates into two consecutive phases (Table S1). This model is presented in the paper. It is based on the assumed direct chronological relationship between mound 2 and 4. The separation of the radiocarbon determinations in their respective kurgan with a prior belief (model A) results in a slightly more precise age probability. The darker grey areas show the calculated age ranges of the model.

B) Model with one phase.

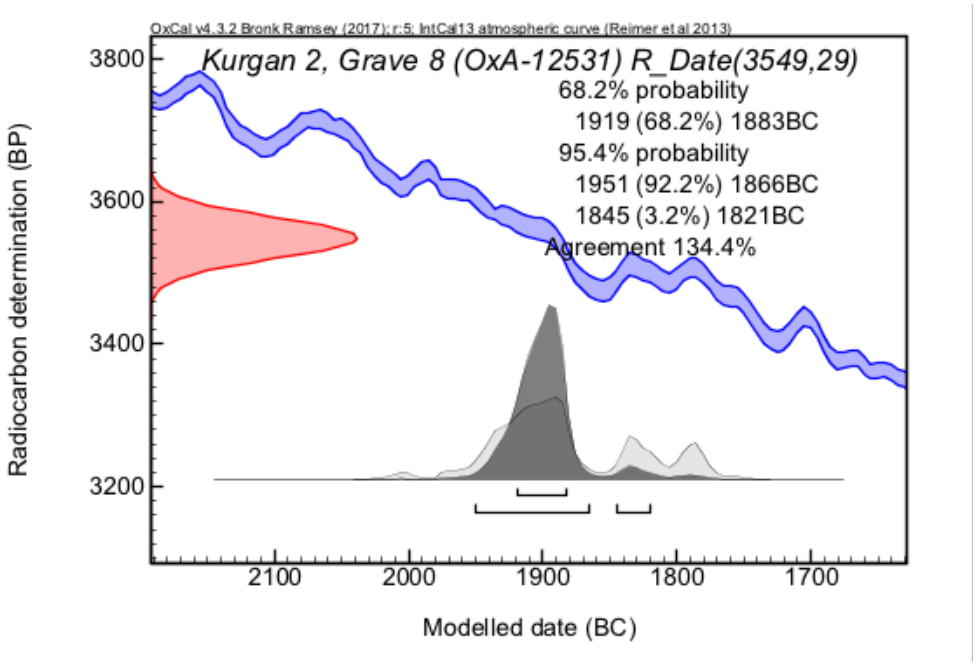

Figure S2. The Bayesian-modelled probable age by incorporating all dates within only one phase (Table S2). Here, the radiocarbon dates are viewed independently from the kurgans. The darker grey areas show the calculated age ranges of the model.

Table S3. Selected stable isotope results for human remains at the KA-5 cemetery; published data from B. Hanks et al. (2018).

Sample No.	Kurgan / grave	$\delta^{13}C$	$\delta^{15}N$	C:N
KA-5 A0995	2 / 6	−18.4	12.6	3.2
KA-5 A0996	2 / 6	−18.5	11.5	3.4
KA-5 A0997	2 / 6	−18.0	12.9	3.1
KA-5 A1000	2 / 6	−17.9	14.9	3.5
KA-5 A1002	2 / 6	−17.7	14.8	3.1

KA-5 A0971	2 / 8	−19.1	11.6	3.5
KA-5 A1008	2 / 8	−18.2	14.2	3.1
KA-5 A1009	2 / 8	−18.3	11.7	3.1
KA-5 A1010	2 / 8	−17.8	13.3	3.3
KA-5 A0983	2 / 12	−17.9	13.4	3.5
KA-5 A0984	2 / 12	−17.4	14.4	3.3
KA-5 A0985	2 / 12	−19.7	11.3	3.1
KA-5 A0986	2 / 12	−19.4	14.8	3.5
KA-5 A0982	2 / 15	−17.8	13.6	3.5
KA-5 A0939	4 / 1	−18.2	12.2	3.47
KA-5 A0937	4 / 3	−17.9	14.24	3.49

Code used for calibrating the radiocarbon dates and the model with two phases in OxCal v4.3

```
Plot()
 {
  Sequence()
  {
   Boundary("Start Phase 1");
   Phase("Kamennyj Ambar 5: Kurgan 2")
   {
    R_Date("Grave 6 (OxA-12530)",  3572, 29);
    R_Date("Grave 15 (OxA-12533)",  3555, 31);
    R_Date("Grave 12 (OxA-12532)",  3604, 31);
    R_Date("Grave 8 (OxA-12531)",  3549, 29);
   };
   Boundary("Transition Phases 1/2");
   Phase("Kamennyj Ambar 5: Kurgan 4")
   {
    R_Date("Grave 3 (OxA-12534)",  3529, 31);
    R_Date("Grave 1 (OxA-12650)",  3521, 28);
    R_Date("Grave 15 (OxA-12535)",  3498, 35);
   };
   Boundary("End Phase 2");
```

```
 };
};
```

Code used for calibrating the radiocarbon ages and the model with one phase in OxCal v4.3

```
Plot()
 {
  Sequence()
  {
   Boundary("Start of 14C series");
   Phase("1")
   {
    R_Date("Kurgan 2, Grave 6 (OxA-12530)",  3572, 29);
    R_Date("Kurgan 2, Grave 15 (OxA-12533)",  3555, 31);
    R_Date("Kurgan 2, Grave 12 (OxA-12532)",  3604, 31);
    R_Date("Kurgan 2, Grave 8 (OxA-12531)",  3549, 29);
    R_Date("Kurgan 4, Grave 3 (OxA-12534)",  3529, 31);
    R_Date("Kurgan 4, Grave 1 (OxA-12650)",  3521, 28);
    R_Date("Kurgan 4, Grave 15 (OxA-12535)",  3498, 35);

   };
   Boundary("End of 14C series");
  };
};
```

References

BRONK RAMSEY, C. 2009. Bayesian analysis of radiocarbon dates. *Radiocarbon* 51: 337–60. https://doi.org/10.1017/S0033822200033865

HANKS, B., A.V. MILLER, M. JUDD, A. EPIMAKHOV, D. RAZHEV & K. PRIVAT. 2018. Bronze Age diet and economy: New stable isotope data from the Central Eurasian steppes (2100–1700 BC). *Journal of Archaeological Science* 97: 14–25. https://doi.org/10.1016/j.jas.2018.06.006

REIMER, P.J. *et al*. 2013. IntCal13 and Marine13 radiocarbon age calibration curves 0–50 000 years cal BP. *Radiocarbon* 55: 1869–87. https://doi.org/10.2458/azu_js_rc.55.16947